Electronic Supporting Information

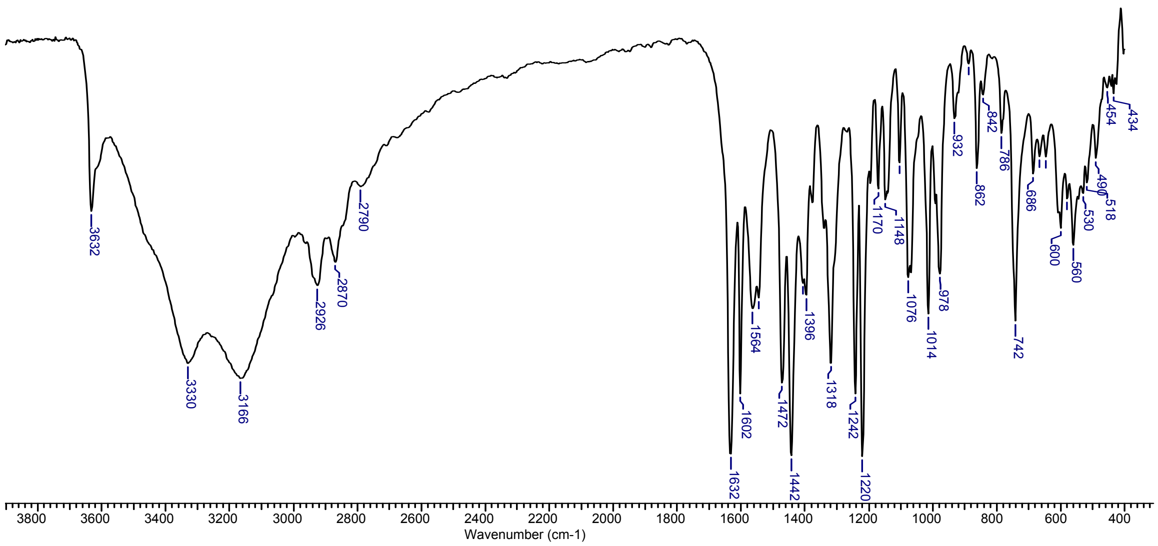

Figure S1. IR transmittance spectrum of **1** in a KBr pellet in the 400–4000 cm^{-1} region

Table S1. Hydrogen bonds for $[Co^{II}Co^{III}(LH_2)_2(H_2O)(CH_3COO)](H_2O)_3$ (**1**) [Å and °]

D-H...A	d(D-H)	d(H...A)	d(D...A)	<(DHA)
O(112)-H(112)...O(213)[1]	0.844(19)	1.85(2)	2.681(3)	168(4)
O(113)-H(113)...O(21)	0.84	2.24	2.946(3)	142.4
O(113)-H(113)...O(26)	0.84	2.34	2.903(3)	124.5
O(212)-H(212)...O(113)[2]	0.856(19)	1.803(19)	2.659(3)	178(4)
O(213)-H(213)...O(16)	0.84	2.30	2.883(3)	126.4
O(213)-H(213)...O(11)	0.84	2.24	2.983(3)	146.8
O(1)-H(1AO)...O(3)	0.796(18)	1.96(2)	2.709(3)	156(4)
O(1)-H(1BO)...O(2)[3]	0.793(18)	1.93(2)	2.709(3)	167(4)
O(2)-H(2AO)...O(4)	0.832(19)	1.85(2)	2.684(3)	175(5)
O(2)-H(2BO)...O(26)	0.806(18)	2.43(3)	3.170(3)	153(5)
O(3)-H(3AO)...O(111)	0.785(18)	2.20(3)	2.862(3)	142(4)
O(3)-H(3BO)...O(32)[4]	0.845(17)	1.945(18)	2.773(3)	166(3)

Symmetry transformations used to generate equivalent atoms: [1] x+1/2,y+1/2,z ; [2] x+1/2,y-1/2,z ; [3] x+1,y,z ; [4] x-1/2,-y+1/2,z-1/2

DC magnetic data and ESR spectra within the spin-Hamiltonian formalism

1) A thorough theoretical analysis for the hexacoordinate Co(II) complexes shows that the spin Hamiltonian formalism fails in the case of an elongated tetragonal bipyramid.[1] In such a case the octahedral $^4T_{1g}$ electronic term splits into the ground ^4E_g and excited $^4A_{2g}$ terms; the axial crystal field splitting parameter is $\Delta_{ax} < 0$ (Figure S2). The spin-orbit coupling causes a further splitting of the ground ^4E_g term into four Kramers doublets (crystal-field multiplets). The analysis of the wave function allows an assignment of the irreducible representations in the corresponding double group D'$_4$. Important is the order of energy levels: Γ_6, Γ_6, Γ_7 and Γ_7 (Bethe notation). This strictly contradicts the assumption of the spin Hamiltonian formalism for which the only two Kramers doublets are Γ_6 (ground, $M_S = \pm 1/2$) and Γ_7 (excited, $M_S = \pm 3/2$) with the energy separation of $2D$ (this applied for a compressed tetragonal bipyramid).

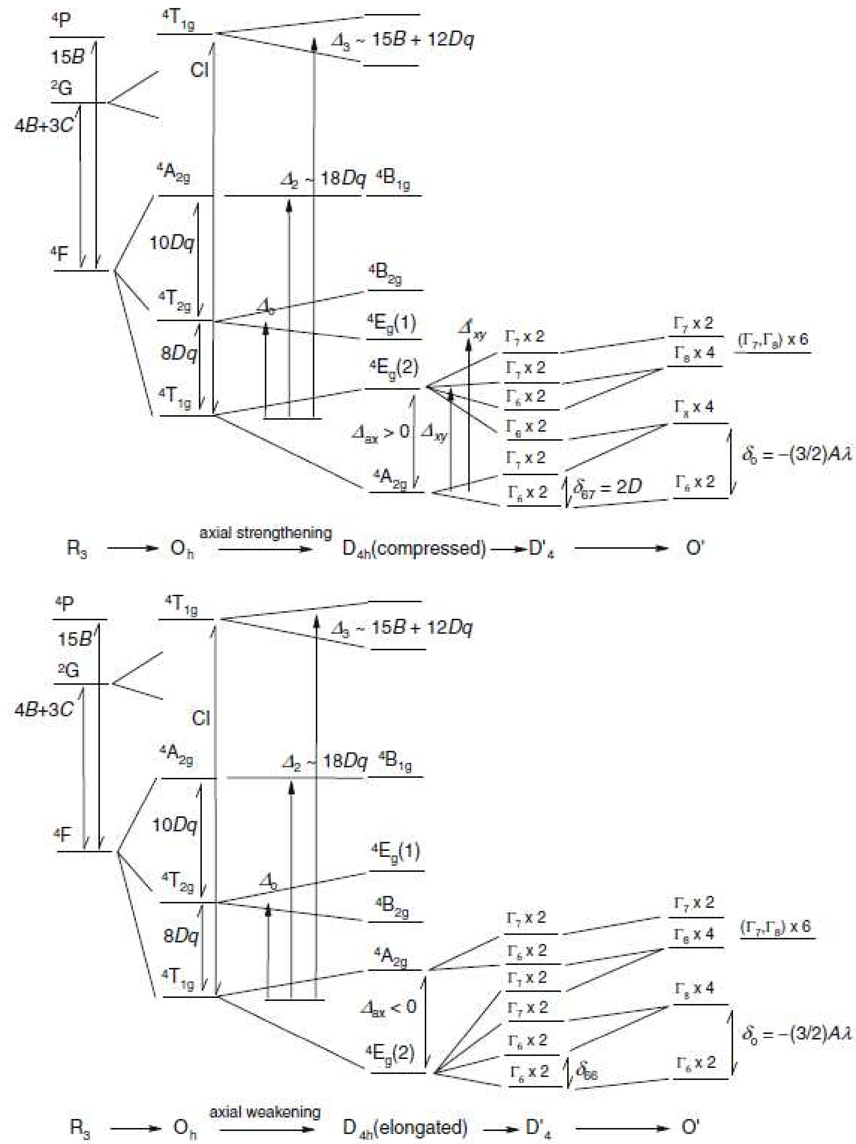

Figure S2. Energy levels of nearly-octahedral d^7 systems on symmetry lowering (not to scale).

(1) Boča, R. Magnetic Parameters and Magnetic Functions in Mononuclear Complexes Beyond the Spin-Hamiltonian Formalism. *Struct. Bonding,* **2006**, *117*, 1-260.

Traditional spin Hamiltonian (ZFS) in the form appropriate to the mononuclear Co(II) $S = 3/2$ systems reads

$$\hat{H}_{k,l} = D(\hat{S}_z^2 - \vec{S}^2/3)\hbar^{-2} + \mu_B B_m (g_x \hat{S}_x \sin\vartheta_k \cos\varphi_l + g_y \hat{S}_y \sin\vartheta_k \sin\varphi_l + g_z \hat{S}_z \cos\vartheta_k)\hbar^{-1} \qquad \text{(S1)}$$

where D is the zero-field splitting parameter and the second contribution is the spin Zeeman term for directions defined by the polar angles $\{\vartheta_k, \varphi_l\}$. The free magnetic parameters cover the axial zero-field splitting parameter D, the magnetogyric factors g_z and $g_x = g_y$. The above Hamiltonian can be safely used in analyzing the magnetic and ESR data for tetracoordinate Co(II) complexes as well as to the subgroup of hexacoordinate complexes exhibiting an axial compression where the ground state is orbitally non-degenerate. Some secondary corrections are represented by the molecular-field correction (zj), and the temperature-independent magnetism χ_{TIM} according to the formula $\chi_{corr} = \chi_{mol}/[1-(zj/N_A\mu_0\mu_B^2)\chi_{mol}] + \chi_{TIM}$. The matrices of the spin Hamiltonian have been diagonalized and the eigenvalues inserted into the van Vleck formula for the susceptibility and the partition function for the magnetization, respectively. Three working magnetic fields need be used in order to determine the van Vleck coefficients numerically in the vicinity of the reference field.

The magnetic data for **1**, $\chi = f(T; B_0 = 0.1\text{ T})$ and $M = f(B, T_0 = 2\text{ K})$, has been fitted to the above Hamiltonian yielding the following set of magnetic parameters: D/hc = 145 cm^{-1}, g_z = 2.357, g_x = 2.872, zj/hc = –0.069 cm^{-1}, and χ_{TIM} = –21 × 10^{-9} m^3 mol^{-1}. The quality of the fit is good as expressed by discrepancy factors for the susceptibility $R(\chi)$ = 0.045 and magnetization $R(M)$ = 0.009 (Figure S3). Attempts to fit the magnetic data with D < 0 failed. Involvement of the E-parameter brought some correlation with D showing an overparametrization for the given experimental dataset.

Despite a good quality of the fit, this set of magnetic parameters is virtual.

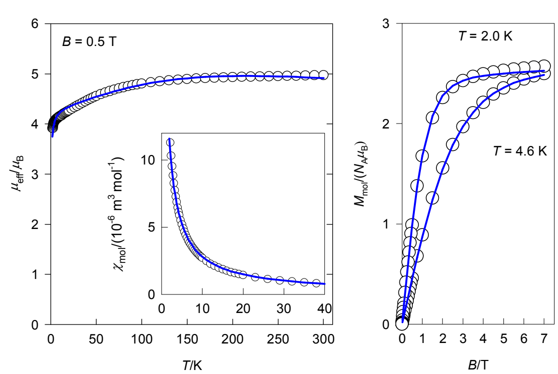

Figure S3. DC magnetic data for **1**. Left – temperature dependence of the effective magnetic moment (inset – temperature dependence of the molar magnetic susceptibility), right – field dependence of the magnetization per formula unit. Open symbols – experimental data, lines – fitted with the ZFS model.

2) If the spin Hamiltonian is applied to an $S = 3/2$ state, the features observed in the ESR spectrum can be simulated assuming certain intrinsic g values associated with certain E/D ratio (with a very large D, of

hundreds of wavenumbers). For each E/D ratio, over a wide range, a set of intrinsic g-parameters can be found which will simulate the spectra (and will result in the observed effective g values). As long as the spin Hamiltonian is applicable (which may not be the case here), there is a proportionality between the deviations of the g-components from 2.0023 and the elements of the zero-field splitting tensor. One could thus try to select a set which, to preserve that proportionality, conforms to

$$E/D = (1/2)(g_x - g_y)/(2g_z - g_x - g_y) \qquad \text{(S2)}$$

This yields the intrinsic values of $g_x = 2.40$, $g_y = 2.73$, $g_z = 2.25$ and $E/D = 0.252$. The fact that our effective g values are frequency-independent up to 634 GHz (corresponding to 21 cm^{-1}) allows us to put a lower limit on the D value, of some 60 cm^{-1}. Above this value, the *effective* g values do not depend on D.

3) As a comparison, the magnetization data and the low-temperature susceptibility data were also fitted by considering an effective spin Hamiltonian for $S^* = 1/2$ and the results are presented in Figure S4. One can see that the principal values of the **g**-tensor are in a reasonable agreement with those observed in EPR.

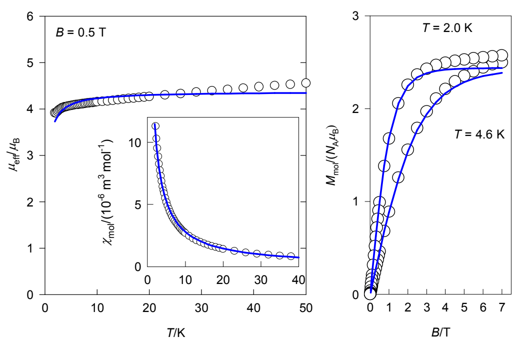

Figure S4. Fit of the DC magnetic data for **1** with the parameters of the *effective* spin $S^* = 1/2$: $g_x = 7.06$, $g_y = 4.20$, $g_z = 2.00$ (EPR data $g_x = 7.18$, $g_y = 2.97$, $g_z = 1.96$.)

Generalized crystal field theory

In the basis set of atomic terms five matrices are constructed and combined to the final interaction matrix: 1. the interelectron repulsion (parametrized by the Racah B and C); 2. the crystal field strength (parametrized by the crystal field poles $F_n(R)$, not to be confused with the Slater-Condon parameters; $10Dq = (10/6)F_4$ in the octahedron); 3. the spin-orbit coupling (parametrized by the true spin-orbit coupling constant ξ); 4. the orbital Zeeman term (accompanied with the orbital reduction factors κ and dependent upon magnetic field B); and 5. the spin Zeeman term (with the true electronic g-factor and B). With 1 + 2 the eigenvalues refer to the crystal field terms; with 1 +2 +3 the eigenvalues are the crystal field multiplets; with 1 + 2 + 3 + 4 + 5 the eigenvalues are the Zeeman levels in the magnetic field. Crystal field terms are classified according to the irreducible representations of the ordinary point groups (Mulliken notation) whereas the crystal field multiplets are classified according to the irreducible representations of the double group (Bethe notation).[1]

(1) Boča, R. Magnetic Parameters and Magnetic Functions in Mononuclear Complexes Beyond the Spin-Hamiltonian Formalism. *Struct. Bonding,* **2006**, *117*, 1–260.

Input for ORCA Program Version 3.0.3 - RELEASE

```
| 86> $new_job
| 87> ! ZORA DefBas2 TightSCF RIJCOSX Grid4 GridX4 NoPop
| 88> ! moread
| 89> %moinp "input.qro"
| 90> %casscf  nel 7
| 91>        norb 5
| 92>        switchstep kdiis
| 93>        mult 4,2
| 94>        nroots 10,40
| 95>        trafostep rimo
| 96>        NEVPT2 true
| 97>        rel
| 98>        dosoc true
| 99>        gtensor true
|100>         printlevel 3
|101> end
|102> end
|103> * xyz 0 4
|104> Co     3.737597    3.904811    9.166505
|105> Co     6.731841    3.904941    9.165790
|106> C      1.988839    4.384915   11.362888
|107> O      2.437861    3.510013   10.488016
|108> C      2.291589    5.765929   11.394422
|109> C      1.686436    6.602080   12.373978
|110> H      1.893200    7.529258   12.387912
|111> C      0.805633    6.091027   13.301834
|112> H      0.401951    6.665799   13.940755
|113> C      0.507171    4.721716   13.300001
|114> H     -0.100360    4.368010   13.937088
|115> C      1.097881    3.886866   12.371961
|116> O      0.903768    2.520416   12.262511
|117> C      0.030254    1.899870   13.205767
|118> H      0.376854    2.037711   14.111256
|119> H     -0.023231    0.938882   13.018582
|120> H     -0.862974    2.296489   13.134083
|121> C      3.169515    6.382314   10.427332
|122> H      3.287608    7.323796   10.483066
|123> N      3.804185    5.761508    9.497277
|124> C      4.618388    6.526657    8.499204
|125> C      4.993187    5.530559    7.382880
|126> H      4.297428    5.547464    6.678875
|127> H      5.851865    5.806241    6.970377
|128> O      5.117732    4.206111    7.896583
|129> C      5.857864    7.084525    9.171675
|130> H      6.316266    7.711313    8.558054
|131> H      5.599210    7.582574    9.986230
|132> O      6.744572    6.014044    9.520377
|133> H      7.452826    6.332899    9.845062
|134> C      3.795288    7.659297    7.889433
|135> H      3.705989    8.386215    8.554387
|136> H      4.279843    8.023406    7.106045
|137> O      2.487545    7.239791    7.476197
```

```
|138> H    2.522103   6.448634   7.197712
|139> C    1.903503   3.462939   7.032894
|140> O    2.405943   4.322496   7.880633
|141> C    2.205517   2.080624   6.981561
|142> C    1.551173   1.240572   6.044355
|143> H    1.751794   0.313394   6.026205
|144> C    0.625837   1.752926   5.160316
|145> H    0.188341   1.178153   4.543029
|146> C    0.332996   3.123537   5.174433
|147> H   -0.293365   3.479844   4.555862
|148> C    0.949739   3.955786   6.083772
|149> O    0.730864   5.314434   6.197622
|150> C   -0.055617   5.955786   5.188183
|151> H    0.355803   5.806241   4.310194
|152> H   -0.097726   6.918075   5.369867
|153> H   -0.961706   5.581274   5.193866
|154> C    3.111101   1.443433   7.909050
|155> H    3.225293   0.503251   7.830216
|156> N    3.773109   2.044213   8.832872
|157> C    4.603337   1.266580   9.808212
|158> C    5.007421   2.263979  10.918119
|159> H    4.319936   2.262679  11.628907
|160> H    5.865846   1.979194  11.320905
|161> O    5.144618   3.579454  10.398182
|162> C    5.840383   0.703511   9.117041
|163> H    6.305987   0.075423   9.724061
|164> H    5.573300   0.208062   8.301386
|165> O    6.716607   1.780624   8.766139
|166> H    7.387382   1.456437   8.341719
|167> C    3.784150   0.135891  10.430816
|168> H    3.670525  -0.583875   9.760728
|169> H    4.287341  -0.240572  11.196237
|170> O    2.497869   0.553966  10.883652
|171> H    2.532224   1.358908  11.121070
|172> O    8.345979   3.660598  10.373249
|173> O    9.693214   3.475942  12.125927
|174> C    8.583030   3.777633  11.622673
|175> C    7.494258   4.291287  12.545396
|176> H    6.696866   4.512353  12.019409
|177> H    7.810217   5.093628  13.011249
|178> H    7.269820   3.599480  13.201917
|179> O    7.961535   4.137191   7.473631
|180> H    7.708749   3.667100   6.880543
|181> H    8.752684   4.096229   7.535048
|182> *
|183>
|184>                  ****END OF INPUT****
```

Elena A. Buvaylo, Vladimir N. Kokozay, Olga Yu. Vassilyeva, Brian W. Skelton, Andrew Ozarowski, Ján Titiš, Beáta Vranovičová, Roman Boča

AC susceptibility data

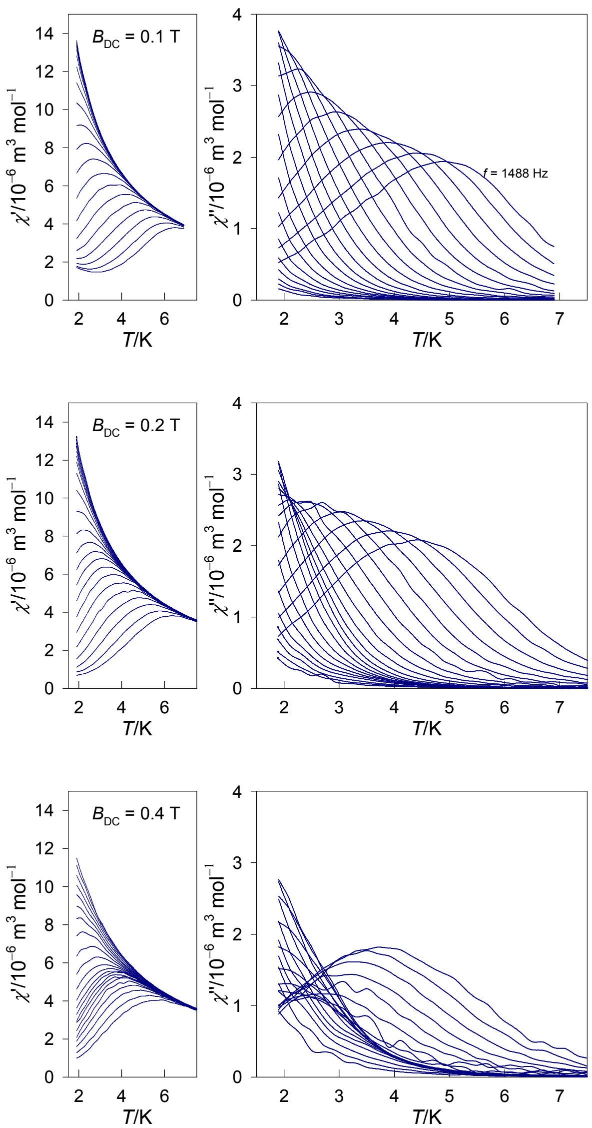

Figure S5. Temperature dependence of the AC susceptibility components for **1** for frequencies *f* = 0.1, 0.16, 0.25, 0.40, 0.63, 1.01, 1.58, 2.51, 3.98, 6.31, 10.01, 15.86, 25.11, 39.81, 63.09, 100.1, 158.4, 251.3, 398.9, 629.2, 997.3 and 1488 Hz.

Two-set Debye model for AC susceptibility:
a) in phase susceptibility

$$\chi'(\omega) = \chi_S + (\chi_{T1} - \chi_S)\frac{1+(\omega\tau_1)^{1-\alpha_1}\sin(\pi\alpha_1/2)}{1+2(\omega\tau_1)^{1-\alpha_1}\sin(\pi\alpha_1/2)+(\omega\tau_1)^{2-2\alpha_1}} + (\chi_{T2} - \chi_{T1})\frac{1+(\omega\tau_2)^{1-\alpha_2}\sin(\pi\alpha_2/2)}{1+2(\omega\tau_2)^{1-\alpha_2}\sin(\pi\alpha_2/2)+(\omega\tau_2)^{2-2\alpha_2}}$$

b) out of phase susceptibility

$$\chi''(\omega) = (\chi_{T1} - \chi_S)\frac{(\omega\tau_1)^{1-\alpha_1}\cos(\pi\alpha_1/2)}{1+2(\omega\tau_1)^{1-\alpha_1}\sin(\pi\alpha_1/2)+(\omega\tau_1)^{2-2\alpha_1}} + (\chi_{T2} - \chi_{T1})\frac{(\omega\tau_2)^{1-\alpha_2}\cos(\pi\alpha_2/2)}{1+2(\omega\tau_2)^{1-\alpha_2}\sin(\pi\alpha_2/2)+(\omega\tau_2)^{2-2\alpha_2}}$$

for $\omega = 2\pi f$. α – the distribution parameter (α = 0 for an ideal system). χ_{T1}, χ_{T2} – isothermal (low-frequency) susceptibilities. χ_S – adiabatic (high-frequency) susceptibility = 0 in the present case.

Elena A. Buvaylo, Vladimir N. Kokozay, Olga Yu. Vassilyeva, Brian W. Skelton, Andrew Ozarowski, Ján Titiš, Beáta Vranovičová, Roman Boča

Table S2. Result of the fitting procedure for AC susceptibility components of **1**

a) at B_{DC} = 0.1 T with a single Debye component

T/K	$R(\chi')$/%	$R(\chi'')$/%	χ_S	χ_{T1}	α_1	τ_1 /10^{-3} s
1.9	1.6	5.9	1.39(8)	13.68(6)	0.25(1)	5.40(13)
2.1	1.3	5.3	1.23(7)	12.37(4)	0.25(1)	3.74(8)
2.3	1.2	4.8	1.11(7)	11.42(4)	0.25(1)	2.76(5)
2.5	0.85	3.9	0.97(5)	10.51(2)	0.25(1)	2.01(3)
2.7	0.77	3.4	0.95(5)	9.75(2)	0.24(1)	1.51(2)
2.9	0.56	2.5	0.86(4)	9.08(1)	0.23(1)	1.13(1)
3.1	0.33	1.8	0.77(2)	8.52(1)	0.23(1)	0.879(7)
3.3	0.32	1.9	0.74(3)	8.02(1)	0.22(1)	0.688(6)
3.5	0.41	2.0	0.69(3)	7.58(1)	0.21(1)	0.543(6)
3.7	0.47	2.3	0.73(4)	7.18(1)	0.20(1)	0.444(5)
4.1	0.55	2.8	0.77(5)	6.51(1)	0.16(1)	0.298(5)
4.5	0.67	3.6	0.79(8)	5.94(1)	0.13(1)	0.195(5)
4.9	0.36	3.6	1.00(7)	5.48(1)	0.09(1)	0.146(3)
5.5	0.30	2.6	1.00(8)	4.90(1)	0.05(1)	0.085(2)
6.1	0.24	2.4	0.93(12)	4.43(1)	0.03(1)	0.051(2)

b) at B_{DC} = 0.2 T with two-set Debye model

T/K	$R(\chi')$/%	$R(\chi'')$/%	χ_{T1}	α_1	τ_1 /10^{-3} s	χ_{T2}	α_2	τ_2 /10^{-3} s
1.9	1.2	5.1	7.42(117)	0.29(3)	23.9(44)	13.28(6)	0.32(3)	1.37(39)
2.1	0.82	3.8	5.00(51)	0.22(3)	24.1(26)	11.99(5)	0.29(2)	1.33(14)
2.3	0.91	3.7	4.16(59)	0.28(4)	21.1(34)	11.17(5)	0.28(2)	1.03(11)
2.5	0.59	2.8	3.24(30)	0.25(3)	17.8(21)	10.31(3)	0.26(1)	0.803(46)
2.7	0.53	2.6	2.50(32)	0.31(3)	15.5(30)	9.57(3)	0.25(1)	0.664(34)
2.9	0.42	2.1	1.86(30)	0.38(4)	14.7(43)	8.97(3)	0.25(1)	0.563(22)
3.1	0.26	0.95	1.35(20)	0.42(3)	12.8(39)	8.42(2)	0.25(1)	0.473(10)
3.3 a	0.36	1.6	1.37(56)	0.50(6)	7.50(762)	7.94(3)	0.23(2)	0.367(9)
3.3 b	0.34	1.5	1.30(49)	0.50(6)	8.38(780)	7.94(3)	0.23(2)	0.370(9)
3.3 c	0.35	1.5	1.71(55)	0.53(2)	4.15(328)	7.95(2)	0.21(2)	0.366(7)
3.5	0.35	1.9	1.38(28)	0.63(3)	2.00(126)	7.54(3)	0.21(1)	0.330(5)
3.7	0.53	2.7	1.72(47)	0.61(6)	0.510(218)	7.12(4)	0.17(2)	0.275(7)
4.1	0.72	3.5	-	-	-	6.33(1)	0.22(1)	0.184(2)
4.5	0.70	3.3	-	-	-	5.81(1)	0.19(1)	0.124(1)
4.9	0.53	4.3	-	-	-	5.36(1)	0.15(1)	0.0878(10)
5.5	0.26	5.5	-	-	-	4.81(1)	0.09(1)	0.0550(7)
6.1	0.37	5.5	-	-	-	4.35(1)	0.06(1)	0.0347(5)

c) at B_{DC} = 0.4 T with two-set Debye model

T/K	$R(\chi')$/%	$R(\chi'')$/%	χ_{T1}	α_1	τ_1 /10^{-3} s	χ_{T2}	α_2	τ_2 /10^{-3} s
1.9	1.7	5.6	9.37(27)	0.34(2)	60.5(28)	11.84(11)	0.28(6)	0.182(28)
2.1	1.7	5.7	8.49(26)	0.37(2)	51.3(28)	11.19(11)	0.22(5)	0.166(19)
2.3	1.3	4.9	7.35(22)	0.38(2)	46.8(24)	10.57(8)	0.25(4)	0.172(14)
2.5	1.2	5.1	5.91(18)	0.35(2)	42.2(23)	9.76(7)	0.26(3)	0.175(12)
2.7	1.0	4.5	5.09(18)	0.38(2)	37.6(23)	9.24(6)	0.26(2)	0.159(9)
2.9	0.74	3.9	4.23(13)	0.38(2)	31.8(18)	8.64(4)	0.24(2)	0.140(5)
3.1	0.66	3.5	3.29(11)	0.38(2)	35.2(21)	8.15(4)	0.25(1)	0.135(4)
3.3	0.52	2.5	2.70(8)	0.41(2)	42.1(24)	7.78(3)	0.25(1)	0.118(2)
3.5	0.60	3.3	1.91(8)	0.38(3)	61.6(46)	7.38(4)	0.27(1)	0.115(2)
3.7	0.46	2.5	1.40(5)	0.34(2)	77.4(46)	6.95(3)	0.27(1)	0.0987(13)
4.1	0.48	1.7	0.80(3)	0.28(3)	110(8)	6.32(2)	0.26(1)	0.0727(8)
4.5	0.37	2.6	0.50(3)	0.27(4)	135(13)	5.81(2)	0.23(1)	0.0513(11)
4.9	0.38	4.3	0.31(3)	0.25(1)	142(23)	5.35(2)	0.19(1)	0.0391(6)
5.5	0.50	4.1	0.17(3)	0.25(12)	200(61)	4.80(2)	0.15(1)	0.0260(6)
6.1	0.23	3.1	0.098(12)	0.25(9)	200(47)	4.37(1)	0.12(1)	0.0169(6)